

Diversification of giant and large eukaryotic dsDNA viruses predated the origin of modern eukaryotes

Julien Guglielmini¹, Anthony Woo², Mart Krupovic², Patrick Forterre^{2*}, Morgan Gaia^{2*}

¹HUB Bioinformatique et Biostatistique, C3BI, USR 3756 IP CNRS, Institut Pasteur, Paris, France

²Unité de Biologie Moléculaire du Gène chez les Extrêmophiles (BMGE), Département de Microbiologie, Institut Pasteur, Paris, France

*corresponding authors:

Patrick Forterre: patrick.forterre@pasteur.fr

Morgan Gaia: morgan.gaia@pasteur.fr

1 **Diversification of giant and large eukaryotic dsDNA viruses predated the origin of**
2 **modern eukaryotes**

3 Julien Guglielmini¹, Anthony Woo², Mart Krupovic², Patrick Forterre², Morgan Gaia²

4

5 ¹HUB Bioinformatique et Biostatistique, C3BI, USR 3756 IP CNRS, Institut Pasteur, Paris, France

6 ²Unité de Biologie Moléculaire du Gène chez les Extrêmophiles (BMGE), Département de

7 Microbiologie, Institut Pasteur, Paris, France

8

9 **Abstract**

10 Giant and large eukaryotic double-stranded DNA viruses from the Nucleo-Cytoplasmic
11 Large DNA Virus (NCLDV) assemblage represent a remarkably diverse and potentially
12 ancient component of the eukaryotic virome. However, their origin(s), evolution and
13 potential roles in the emergence of modern eukaryotes remain a subject of intense
14 debate. Since the characterization of the mimivirus in 2003, many big and giant viruses
15 have been discovered at a steady pace, offering a vast material for evolutionary
16 investigations. In parallel, phylogenetic tools are constantly being improved, offering
17 more rigorous approaches for reconstruction of deep evolutionary history of viruses
18 and their hosts. Here we present robust phylogenetic trees of NCLDVs, based on the 8
19 most conserved proteins responsible for virion morphogenesis and informational
20 processes. Our results uncover the evolutionary relationships between different NCLDV
21 families and support the existence of two superclades of NCLDVs, each encompassing
22 several families. We present evidence strongly suggesting that the NCLDV core genes,
23 which are involved in both informational processes and virion formation, were acquired
24 vertically from a common ancestor. Among them, the largest subunits of the DNA-
25 dependent RNA polymerase were seemingly transferred from two clades of NCLDVs to

26 proto-eukaryotes, giving rise to two of the three eukaryotic DNA-dependent RNA
27 polymerases. Our results strongly suggest that these transfers and the diversification of
28 NCLDVs predated the emergence of modern eukaryotes, emphasizing the major role of
29 viruses in the evolution of cellular domains.

30

31

32 The discovery of giant viruses in the early 21st century has revived the debate on
33 the nature of viruses and their role in evolution¹⁻¹³. The 1µm-long particles of
34 pithoviruses¹⁴ can be seen under a light microscope and the 2.5Mb-long genomes of
35 pandoraviruses, larger than those of many cellular organisms, encode for more than
36 2,000 proteins, mostly ORFans¹⁵. However, these unexpected features notwithstanding,
37 giant viruses are a *bona fide* part of the virosphere, relying on the infected cells for the
38 production of energy and protein synthesis. Phylogenetic and comparative genomics
39 analyses showed that giant viruses together with smaller eukaryotic dsDNA viruses
40 form a supergroup, dubbed the Nucleo-Cytoplasmic Large DNA Viruses (NCLDV)^{16,17}.
41 This assemblage encompasses families of large and giant viruses, including *Poxviridae*,
42 *Iridoviridae*, *Ascoviridae*, *Asfarviridae*, *Marseilleviridae*, *Mimiviridae*, and *Phycodnaviridae*
43 as well as several lineages of as yet unclassified viruses, such as pithoviruses,
44 pandoraviruses, molliviruses and faustoviruses¹⁸. Altogether, the NCLDVs are associated
45 with diverse eukaryotic phyla, from phagotrophic protists to insects and mammals, and
46 some cause devastating diseases, such as smallpox (*Poxviridae*) or swine fever
47 (*Asfarviridae*), or play important ecological roles, such as termination of algal blooms
48 (*Phycodnaviridae*¹⁹).

49

50 The origin and evolution of the NCLDVs remain a subject of controversy. It is still
51 unclear if these viruses form a monophyletic group, if proteins conserved in most
52 NCLDVs had a congruent evolutionary history or if some of them were acquired several
53 times independently from their hosts. Most phylogenetic analyses performed up to now
54 were based on individual proteins or various subsets of conserved proteins^{20,21}. These
55 analyses usually recovered the monophyly of various NCLDV families, but often offered
56 contradicting results and the relationships between the families remained debated. For
57 instance, it has been proposed that the giant pandoraviruses are related to members of
58 the *Phycodnaviridae*²², but this grouping was not recovered in a recent phylogeny based
59 on their DNA polymerases²³. According to some studies, the different families of the
60 NCLDVs emerged during the diversification of modern eukaryotes²⁴, whereas in other
61 studies, NCLDVs form a monophyletic group branching between Archaea and
62 Eukarya²⁹/10/2018 13:51:00. Some authors have even suggested that several families
63 of giant viruses could have originated independently from extinct cellular lineages,
64 possibly even before the last universal common ancestor (LUCA) of Archaea, Bacteria,
65 and Eukarya^{11,25}.

66

67 With phylogenetic tools being constantly improved and new genomes of large
68 and giant viruses steadily unearthed, we decided to perform an updated and in-depth
69 phylogenetic analysis of the NCLDVs. We mined available genomes for homologous
70 genes, built clusters of orthologous genes, and performed extensive phylogenetic
71 analyses on the 8 most conserved ones, separately and in concatenations. In addition,
72 we have investigated the relationships between NCLDVs and eukaryotes through the
73 phylogeny of the DNA-dependent RNA polymerases (RNAP). Unlike in previous
74 analyses, we included in our study the three eukaryotic RNAP (RNAP I, II, and III) and

75 concatenated their two largest subunits. The robust phylogenies we obtained show that
76 core genes involved in virion morphogenesis as well as genome transcription and
77 replication have co-evolved in the entire NCLDV lineage. Furthermore, our results
78 revealed the existence of two superclades of NCLDVs that diverged after the separation
79 of the archaeal and eukaryotic lineages, but before the emergence of the Last Eukaryotic
80 Common Ancestor (LECA). Surprisingly, our data suggest that eukaryotic RNAP-III is the
81 actual cellular ortholog of the archaeal and bacterial RNAP, while eukaryotic RNAP-II
82 and possibly RNAP-I were transferred between two viral families and proto-eukaryotes.
83 Overall, our results reveal that the diversification of NCLDVs predates the origin of
84 modern eukaryotes: the ancestors of contemporary NCLDVs co-evolved with proto-
85 eukaryotes and could have played an important role in the emergence and
86 diversification of modern eukaryotes.

87

88 **Results**

89 **Identification of the core genes**

90 Many new NCLDV genomes have been published following the latest
91 comprehensive comparative genomics analyses^{21,26}, substantially increasing their
92 known diversity and enriching families that were previously poorly represented. As a
93 result, the list of the most conserved genes among the NCLDVs could have drastically
94 changed since the last estimation, prompting us to re-analyse it. To identify NCLDV
95 orthologs, we designed a pipeline based on Best Bidirectional BLAST Hit combined with
96 manual curation in order to remain as exhaustive as possible while avoiding inclusion of
97 paralogs (see details in Methods section). The sets of conserved proteins classified
98 according to their conservation among NCLDVs are summarized in Supplementary Table
99 1.

100 Our results show that only 3 proteins are strictly conserved among the 73
101 selected NCLDV genomes: family B DNA polymerase (DNApol B), the D5-like primase-
102 helicase (primase hereinafter) and homologs of the Poxvirus Late Transcription Factor
103 VLTF3 (VLTF3-like) (list of genomes in Supplementary Table 2; selection criteria in
104 Methods). Acknowledging various reasons which may preclude detection of homologous
105 genes (e.g., due to high divergence or genuine loss in a taxon), we decided to lower our
106 conservation threshold to include genes found in at least 95% of the genomes. This
107 resulted in the increase of our set of core genes by three: the transcription elongation
108 Factor II-S (TFIIS), the genome packaging ATPase (pATPase), and the major capsid
109 protein (MCP). Notably, no homolog of the MCP has been found in pandoraviruses¹⁵,
110 whereas pATPases are apparently lacking in Pithovirus¹⁴, Cedratvirus²⁷, and
111 Orpheovirus²⁸. Conservation of the NCLDV genes is further discussed in the
112 Supplementary Information.

113

114 To this set of six proteins (3 strictly conserved and 3 conserved in 95% of the
115 genomes), we added the two largest RNAP subunits (RNAP-a and -b) despite their
116 notable absence in all genera of the *Phycodnaviridae* family, except for the
117 *Coccolithovirus* genus. Indeed, these two proteins are otherwise highly conserved among
118 the NCLDVs (present in 92% of the genomes) and are the largest universal markers
119 (found in all members of the three cellular domains), which makes them perfectly suited
120 for reconstructing the evolutionary relationships between NCLDVs and cellular
121 organisms. Thus, the set of 8 proteins contains 6 proteins related to informational
122 processes – genomes expression and replication (DNApol B, primase, VLTF3-like, TFIIS,
123 RNAP-a, and RNAP-b) – and 2 proteins involved in virion structure and morphogenesis
124 (pATPase and MCP).

125

126 **The core markers share a similar phylogenetic signal**

127 Using a maximum-likelihood (ML) framework, the monophyly of all known
128 NCLDV families, except the *Phycodnaviridae*, was obtained with high support in most of
129 the 8 single-protein phylogenetic trees (Supplementary Figure 1). As often observed in
130 published NCLDV phylogenies²⁶, *Ascoviridae* were however nested within the
131 *Iridoviridae* in most trees. The grouping of the *Mimiviridae* with related unclassified
132 viruses with smaller genomes often referred to as the “extended Mimiviridae”²¹ or more
133 recently the “Mesomimivirinae”²⁹, was obtained in five out of the 8 trees. We will refer
134 to this grouping as the “Megavirales” putative order (see Supplementary Information).

135

136 The *Poxviridae* clade consistently formed a long branch and displayed the most
137 unstable position, branching next to various families (see Supplementary Information).
138 The same was true for *Aureococcus anophagefferens* virus. Thus, to avoid potential
139 artefacts, we decided to remove these taxa from most of our subsequent analyses.
140 Phylogenetic analyses of the resultant dataset resulted in globally congruent trees of
141 individual core proteins (Supplementary Figure 2). Notably, the *Marseilleviridae*, the
142 *Ascoviridae*, the *Iridoviridae*, and a clade grouping *Pithovirus sibericum* with *Cedratvirus*
143 A11 and *Orpheovirus IHUM-LCC2* (thereafter referred as the Pitho-like viruses), group
144 seemingly together, while the *Phycodnaviridae* (including *Pandoraviruses* and
145 *Mollivirus*), *Asfarviridae*, and the “Megavirales” also form a cluster.

146

147 In order to verify if the NCLDV informational proteins have indeed co-evolved
148 with proteins involved in virion formation, we first concatenated independently the 4
149 largest informational proteins (i.e. the DNA and RNA polymerases, and the primase) and

150 next the 2 proteins involved in the formation of virions (the MCP and the pATPase). In
151 both trees (Supplementary Figure 3 and 4), all NCLDV families were monophyletic,
152 except for the *Iridoviridae* which again were split by the *Ascoviridae* in the tree
153 constructed from the concatenation of informational proteins (Supplementary Figure 3).
154 The two phylogenies had similar topologies, with the same clusters of NCLDV families as
155 observed in single-protein trees. Some positions within these clusters might be affected
156 by differences between the two datasets: 2 of the 4 informational proteins are absent in
157 all but one *Phycodnaviridae* genera, while the Pitho-like viruses lack the pATPase gene.
158 The congruence between the two trees still suggests that informational proteins of the
159 NCLDVs have mostly co-evolved with proteins involved in the formation of virions. The
160 8 core genes hence likely underwent through a similar evolutionary history.

161 To further confirm that the 8 core proteins have a similar evolutionary history
162 and to detect potential incongruences within the selected proteins that could prevent
163 their global concatenation, we performed a home-made congruence test based on
164 comparative phylogenetic analyses of differential concatenations (see details in
165 Methods; Supplementary Table 3). The topologies of the resulting trees were congruent,
166 with most features systematically present, such as the two clusters of NCLDV families,
167 the presence of groups regularly observed in the ML trees, and the monophyly of
168 families. This test thus did not reveal any major incongruences between the different
169 combinations of core proteins and consequently strongly supports the absence of
170 conflicting signal embedded in a sequence or in a subset of proteins, confirming that the
171 core proteins were likely presents in a common ancestor of NCLDVs and all evolved
172 vertically along their co-evolution with their hosts.

173

174 **The evolution of NCLDVs**

175 We concatenated the 8 core proteins together to improve the robustness and
176 resolution of the NCLDV phylogeny. We obtained a ML tree (Supplementary Figure 5) in
177 which the NCLDV families are again clustering into two superclades: the *Marseilleviridae*
178 with the *Ascoviridae*, the Pitho-like viruses' clade, and the *Iridoviridae* (thereinafter
179 referred as the MAPI superclade), and the *Phycodnaviridae* with the *Asfarviridae* and the
180 "Megavirales" (thereinafter referred as the PAM superclade). All positions in this tree
181 are strongly supported except for the position of the *Asfarviridae* (see Supplementary
182 Information). We further performed Bayesian inferences with the CAT-GTR model,
183 designed to deal with sites and sequences heterogeneity, considering that this could
184 allow a more trustful and accurate reconstruction provided that a satisfactory
185 convergence could be obtained (see Methods). After reaching a good convergence
186 (maxdiff <0.1), we obtained a phylogenetic tree with all nodes at maximum support
187 (Posterior Probabilities = 1), except for two nodes corresponding to minor internal
188 positions within the *Mimiviridae* family. The Bayesian tree was almost identical to the
189 ML tree, except that *Phycodnaviridae* are now sister group to a clade clustering
190 *Asfarviridae* and "Megavirales" (Fig 1). This topology was also confirmed using a
191 supertree approach (Supplementary Figure 6; details in Methods and Supplementary
192 Information).

193
194 This tree confidently positions recently identified viruses. The *Mimiviridae* hence
195 include Klosneuvirus, Indivirus, Catovirus, Hokovirus³⁰, and Tupanvirus³¹, and are
196 associated with related viruses within the putative "Megavirales" order. The still
197 unclassified Pitho-like viruses, which herein consists of Pithovirus sibericum,
198 Cedratvirus A11, and Orpheovirus IHUM-LCC2, seem to represent a new separate family
199 whose position within the putative MAPI superclade remains to be investigated to

200 further extent considering their still low representation. Faustovirus^{32,33}, Pacmanvirus³⁴,
201 and Kaumoebavirus³⁵, form a well-supported clade with the African swine fever virus
202 (ASFV-1) of the *Asfarviridae*, as previously suggested³⁶. The *Phycodnaviridae* encompass
203 pandoraviruses and Mollivirus sibericum. The monophyly of this family however
204 remains a matter of debate as it is not observed in half of the single-protein trees and
205 has low support in the ML tree based on the concatenated structural proteins. This is
206 possibly due to the very large diversity of the viruses within this family. Altogether, our
207 in-depth phylogenetic analyses nonetheless strongly support the existence of the two
208 major superclades, the MAPI and the PAM.

209

210 The evolution and origin of NCLDVs is regularly debated, most notably in term of
211 their connections to other viruses¹⁸. Interestingly, homologs of the MCP and pATPase
212 can be found in viruses from various families belonging to the PRD1-Adenovirus lineage.
213 This lineage was initially proposed based on the structural conservation of the major
214 capsid proteins as well as shared principles of virion assembly and genome packaging³⁷⁻
215 ³⁹. The closest outgroup to NCLDVs in this lineage could be Polintoviruses^{40,41}. When
216 using Polintoviruses as an outgroup (see Methods), the ML tree of the MCP-pATPase
217 concatenation is split between the MAPI and PAM putative superclades, suggesting that
218 these two clusters indeed form monophyletic assemblages (Fig 2). Notably, the MCP-
219 pATPase tree remains almost identical to the one obtained with the NCLDVs alone (the
220 only difference being the position of the *Phycodnaviridae*), and the number of positions
221 was not dramatically reduced (601 positions with Polintoviruses versus 625 positions
222 without). This indicates that the split between the MAPI and PAM superclades was
223 probably the earliest event in the evolution of known modern NCLDVs from their
224 common ancestor.

225

226 **The relationship between NCLDV and the three cellular domains**

227 The RNA and DNA polymerases of NCLDV have homologues in the three domains
228 of life (Archaea, Bacteria and Eukarya), making it *a priori* possible to investigate their
229 evolutionary relationships with cellular organisms. However, the family B DNA
230 polymerase, often used to tentatively affiliate new NCLDV genomes to known taxa⁴²,
231 cannot be used for this task since they are absent from most Bacteria and their
232 phylogenetic analyses produce complex scenarios with the two major subgroups of
233 archaeal DNA polymerases intermingled with the four types of eukaryotic family B DNA
234 polymerases (α , δ , ϵ , ζ)⁴³. In contrast, phylogeny of the two largest RNAP subunits,
235 which are also the largest universal markers, recovered the monophyly of the three
236 cellular domains⁴⁴. Thus, RNAPs are good candidates to study the relationships between
237 the cellular domains and NCLDVs.

238

239 Most phylogenetic analyses of RNAPs performed until now included only the
240 eukaryotic RNA polymerase II (RNAP-II), which is the most studied and usually
241 considered as the most similar to the archaeal RNAPs⁴⁵. Here, we decided to include all
242 three eukaryotic RNAPs (RNAP-I, RNAP-II and RNAP-III) (we used a normalized
243 nomenclature, see Supplementary Information). Importantly, these three multi-subunit
244 RNAPs are present in all eukaryotes, indicating that they were already all present in the
245 Last Eukaryotic Common Ancestor (LECA). Their inclusion in our dataset thus should
246 both reduce the length of the eukaryotic branch and provide three universal eukaryotic
247 phylogenies, thus three positions for LECA in the cellular/NCLDV RNAP tree.

248

249 We have previously obtained a robust phylogenetic RNAP tree with a
250 concatenation of the two largest RNAP subunits (in ML and Bayesian frameworks), in
251 which the three domains are monophyletic, with Eukaryotes and Archaea being sister
252 groups (the so-called Woese's tree). We obtained this result using a balanced dataset
253 (same number of species for each of the three domains) and avoiding known fast-
254 evolving species to prevent long branch attraction artefacts^{44,46}29/10/2018 13:51:00.
255 Since our initial dataset included only RNAP-II as the eukaryotic representative, we
256 added the eukaryotic RNAP-I and RNAP-III (list of selected taxa in Supplementary Table
257 4). Interestingly, Archaea and Eukarya again form two monophyletic sister groups in our
258 new concatenated RNAP subunits tree, despite the drastic reduction of the eukaryotic
259 branch length (Supplementary Figure 7). Remarkably, RNAP-I was not attracted by
260 Bacteria despite its very long branch. These observations suggest that the three-domain
261 topology of the RNAP tree did not result from the attraction of eukaryotes by the long
262 bacterial branch. Interestingly, the three eukaryotic RNAPs displayed globally congruent
263 phylogenies, corroborating their presence in LECA.

264
265 We included the sequences of NCLDV into this new dataset (except for
266 *Poxviridae* and *Aureococcus anophagefferens* virus) in order to investigate the timeline of
267 NCLDV diversification in the context of cellular evolution. The ML phylogenetic analysis
268 of concatenated RNAP subunits yielded the three-domain topology (Supplementary
269 Figure 8) in which NCLDV branch after the divergence of the archaeal and eukaryotic
270 lineages. We then removed Bacteria from our subsequent analyses in order to increase
271 the resolution (single-protein trees in Fig 3 and in Supplementary Figure 9;
272 concatenation in Supplementary Figure 10). The trees were highly similar after selecting
273 the Archaea as the outgroup, and supports for several nodes indeed became stronger.

274 Since each of the cellular clades (the Archaea and the three eukaryotic homologs) was
275 well represented and systematically monophyletic, we decided to use the cellular
276 sequences as constraints during the alignment process (each of the 4 clades of cellular
277 sequences corresponding to an independent constraint; see details in Methods),
278 allowing us to check if this could improve the resolution by limiting mis-alignments
279 from small insertions or deletions in the viral sequences. The resulting concatenation of
280 the two subunits switched from 1,683 positions to 1,595, and the highly supported
281 reconstructed tree obtained in ML framework (LG+C60 model) (Fig 4) was strictly
282 identical to the one without any constraint. The most significant feature of the
283 viral/cellular RNAP tree is that LECA, despite being a single timepoint in the history of
284 eukaryotes, is represented three times among the diversity of NCLDVs, indicating that
285 NCLDVs predated LECA. This reveals that the diversification of NCLDVs itself predated
286 that of modern eukaryotes, and consequently, different NCLDV families or superclades
287 were already infecting proto-eukaryotes.

288

289 Surprisingly, in the tree based on concatenated RNAP subunits, the eukaryotic
290 RNAP-III appears to be the closest to the archaeal outgroup after addition of viral
291 sequences with strong supports, suggesting that it could be the actual ortholog of the
292 archaeal enzyme (Fig 4). A major feature of this tree is that NCLDVs do not form a
293 monophyletic group, but three monophyletic subgroups well separated from the three
294 eukaryotic RNAPs, instead of emerging from within eukaryotic diversity. In order to test
295 this result, we performed an Approximately Unbiased (AU) tree topology test and
296 compare this tree to two others constraining either the monophyly of NCLDVs or
297 cellular organisms (see Methods). The AU test rejected these two alternative trees with
298 p-values $<1e-3$. Remarkably, the relative positions of the NCLDV families and

299 superclades in the RNAP tree are completely congruent with the NCLDV topology in the
300 Bayesian tree previously obtained with the 8 core proteins (Fig 1) and highly similar to
301 the tree obtained using the concatenation from which the two RNAP subunits were
302 omitted during the congruence test (Supplementary Table 3; Supplementary Figure 11).
303 In particular, we recovered the monophyly of the MAPI superclade, and its internal
304 phylogeny is highly similar to that obtained previously (the positions of *Marseilleviridae*
305 and Pitho-like viruses are flipped).

306

307 Four clades of the NCLDVs are distinguishable in this viral-cellular RNAP tree,
308 corresponding to the monophyletic MAPI superclade, the *Phycodnaviridae*, the
309 “Megavirales” and the *Asfarviridae*. The PAM superclade is indeed not monophyletic in
310 the RNAP tree because eukaryotic RNAP-I and -II are branching within it. The relative
311 positions of the three PAM families compared to each other are still matching the NCLDV
312 tree topology obtained with the 8 core proteins in the Bayesian framework (Fig 1), but
313 in the viral/cellular RNAP tree, the eukaryotic RNAP-II is sister group to the
314 “Megavirales” whereas the eukaryotic RNAP-I is sister group to *Asfarviridae*. In order to
315 assess the robustness of these groupings, and notably of the *Asfarviridae* and RNAP-I
316 that both display long branches, we reconstructed a consensus bootstrap tree of the
317 concatenated RNAP subunits. In parallel, we also performed a phylogenetic analysis
318 based on reconstructed ancestral sequences to replace the three eukaryotic RNAP clades
319 (see Methods). Both methods supported the relationships between the “Megavirales”
320 and the eukaryotic RNAP-II as well as between the *Asfarviridae* and the eukaryotic
321 RNAP-I, suggesting that they reflect a genuine evolutionary signal (Supplementary
322 Figure 12). Worth-noting, the position of the *Asfarviridae* differs in the two single-
323 protein subunit trees: they are sister group to the RNAP-I in the individual *a* subunit

324 tree (Fig 3a), as in the tree based on concatenated RNAP subunits (Fig 4), whereas they
325 branch within the “Megavirales” in the *b* subunit tree (Fig 3b). This suggests that two
326 transfers might have occurred between proto-eukaryotes and ancestors of the
327 *Asfarviridae* and could explain the long branch of the *Asfarviridae* in the RNAP trees.

328

329 Considering the branching of NCLDVs after the eukaryotic RNAP-III, it seems that
330 they have originally obtained their RNAP from proto-eukaryotes after their divergence
331 from the archaeal lineage. The unexpected positions of RNAP-I and -II within NCLDVs
332 could suggest that these two eukaryotic RNAPs were either recruited from NCLDVs or
333 transferred to the ancestors of the *Asfarviridae* family and “Megavirales” order. The
334 latter hypothesis seems unlikely because replacements of the two largest core genes of
335 two major NCLDV families by their cellular counterparts would have likely resulted in
336 substantial alterations in the NCLDV topologies obtained during the congruence test.
337 This was not the case, and notably, the tree produced without RNAP genes during this
338 test (Supplementary Figure 12) was highly similar with the 8-core-proteins tree (Fig 1),
339 and with the trees from the concatenated RNAP genes only, with (Fig 4) or without cells
340 (Supplementary Figure 13). The only difference is the position of *Phycodnaviridae*,
341 which are sister group to “Megavirales” in the absence of RNAP genes. This is
342 remarkable since the RNAP proteins represent nearly half of the total positions in the
343 global concatenation. These data strongly suggest that the transfers of the RNAP-
344 encoding genes were directed from viruses to cells, after the diversification of these
345 RNAPs within NCLDVs. Based on this observation, we postulate a possible scenario
346 depicted in Fig 5. In this hypothesis, the ancestral eukaryotic RNAP (at least the two
347 largest subunits), more similar to RNAP-III, was first transferred to the ancestor of
348 NCLDVs. After the divergence between the MAPI and the PAM superclades, this viral

349 RNAP diverged in the common ancestor of “Megavirales” and *Asfarviridae*, and was
350 transferred to proto-eukaryotes, later to become the RNAP-II. Separately, a duplication
351 of the ancestral RNAP-III in proto-eukaryotes occurred, before the largest subunit of this
352 newly formed RNAP was replaced by that of *Asfarviridae*: this new complex, partly viral
353 and partly cellular from duplication, resulted in the RNAP-I.

354

355 **Discussion**

356 From our investigation of the NCLDV genomes, including those of most recently
357 identified giant and large dsDNA viruses, we could reconstruct a robust phylogenetic
358 tree of this group likely to represent their vertical evolutionary history. Our results
359 provide a solid framework for proposed and sometimes debated positions of different
360 NCLDV families. Notably, Pithovirus and related viruses form a separate, yet to be
361 named family most closely related to the *Marseilleviridae*. Pandoraviruses and Mollivirus
362 branch within the *Phycodnaviridae*, as a sister group to *Coccolithovirus* genus,
363 confirming the results of Yutin and Koonin²². Our results reveal two robust
364 monophyletic superclades, the MAPI and the PAM, each of which includes several virus
365 families and a number of unclassified viruses. These results call for reassessment of the
366 taxonomy of large and giant dsDNA viruses included in the NCLDV assemblage. In
367 particular, the expansion of the *Mimiviridae* family and discovery of associated but more
368 distantly related viruses suggests that a family-level taxon might not be adequate to
369 encompass this diversity. Consequently, the *Mimiviridae* and the related algal viruses as
370 well as viruses discovered by metagenomics might have to be unified into a new order,
371 the “Megavirales”. Furthermore, the *Asfarviridae* clade, in addition to ASFV-1, includes
372 the Faustovirus^{32,33}, Kaumoebavirus³⁵ and Pacmanvirus³⁴, which have been suggested to
373 represent separate families³⁵. Thus, an order-level taxon would be needed for

374 classification of these viruses. Similarly, in the MAPI superclade, the placement of the
375 pandoraviruses and the mollivirus within the *Phycodnaviridae* indicates that this family
376 might not be monophyletic and should be revised. *Ascoviridae* regularly branch within
377 *Iridoviridae*, advocating for a reconsideration of these two families. The elusive position
378 of the *Poxviridae*, which were removed from most of our analyses, and their actual
379 association to NCLDVs remain to be investigated.

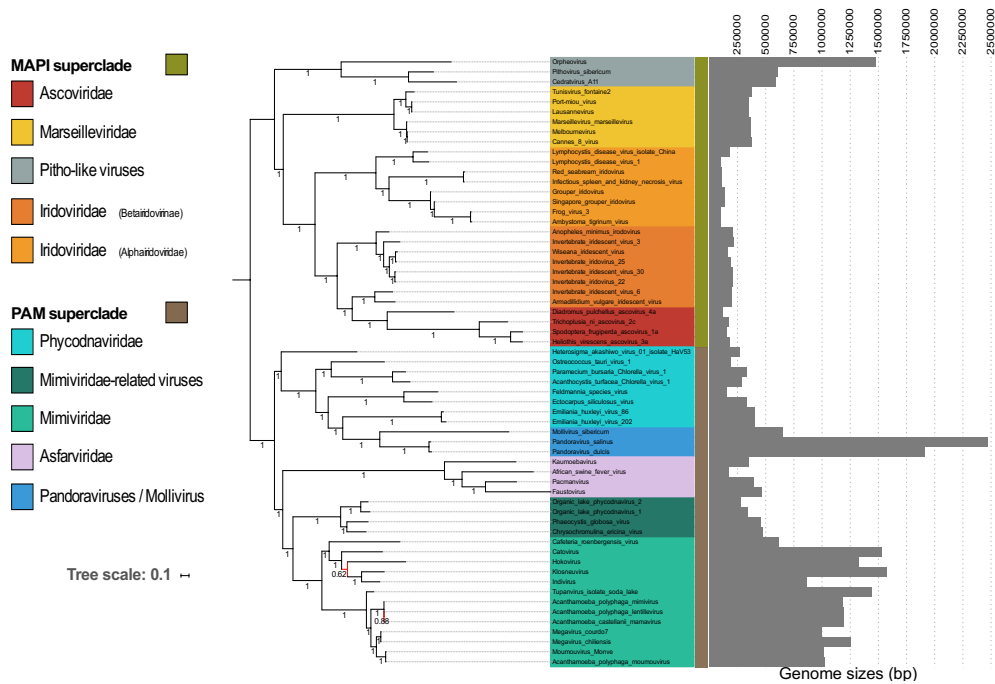
380

381 The monophyly of NCLDVs is not recovered in the cellular/NCLDV RNAP tree:
382 NCLDVs do not form a fourth domain of life, as proposed by some²⁰, nor nest among
383 eukaryotes²⁴. While some genes in the NCLDV genomes might have been recruited from
384 different sources, notably their modern hosts and bacteria, we have shown that a
385 congruent vertical evolutionary history of NCLDVs is traceable and sound. The 8
386 selected core genes selected indeed shared a similar vertical evolution, and were
387 inherited from a common ancestor, which was likely smaller, as hypothesized before⁴⁷,
388 and specifically related to polintoviruses¹². Notably, these core genes are involved in
389 both genome replication and virion formation, key features of viruses, supporting their
390 evolution from a viral ancestor. The division into the two superclades that our results
391 confidently describe seems to have been the most basal event in the evolutionary
392 history from this ancestor toward modern NCLDVs. The MAPI superclade gave rise to
393 *Marseilleviridae*, *Ascoviridae*, Pitho-like viruses, and *Iridoviridae*. The second superclade,
394 PAM, comprises the *Phycodnaviridae*, the *Asfarviridae*, and the “Megavirales”.
395 Interestingly, giant viruses do not cluster together in the NCLDV trees. Most of them are
396 present in the PAM superclade, but in two separate families (*Mimiviridae* and
397 *Phycodnaviridae*), whereas Orpheovirus is present in the MAPI superclade (Fig 1). The
398 scattered distribution of giant viruses within the diversity of NCLDVs strongly opposes a

399 giant – viral or cellular – ancestor scenario as proposed previously^{11,25}. By contrast, it
400 suggests that along the evolution of NCLDVs massive increases in genome size have
401 occurred several times independently in different virus groups, potentially through
402 successive steps of reduction and expansion of their genomes^{48,49}.

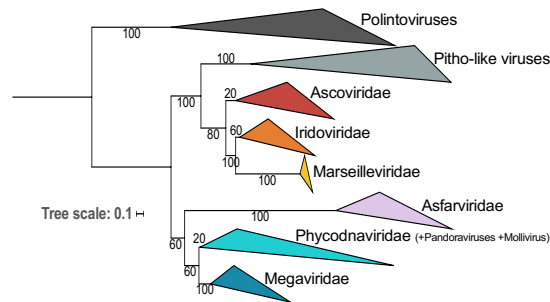
403

404 Our analyses of the two largest subunits of the RNAP, including the three
405 eukaryotic polymerases, revealed that the genuine ortholog of the archaeal and bacterial
406 RNAP might actually be the eukaryotic RNAP-III. In agreement with this unexpected
407 result, homologs of the eukaryotic RNAP-III specific subunit RPC34 are present in most
408 archaeal lineages^{50,51}. Importantly, the inclusion in our analyses of the three eukaryotic
409 polymerases, which emerged and were fixed in the LECA before the emergence of
410 modern eukaryotes, provided a relative timeframe for the NCLDVs' origin and
411 diversification. Our RNAP trees, by positioning the three monophyletic eukaryotic
412 homologs, representing LECA, within the diversity of NCLDV families strongly imply that
413 the evolution of NCLDVs toward the MAPI and PAM superclades and subsequent
414 emergence of the constituent families predated the evolutionary bottleneck that marked
415 the emergence of modern eukaryotes. Several authors have suggested that NCLDVs have
416 played a central role in the origin of eukaryotes^{7,9,52-54}. Our results indeed suggest that
417 modern eukaryotes obtained two of their three RNAP, RNAP-I and RNAP-II from
418 NCLDVs. Preliminary studies also suggested that eukaryotes obtained their major type II
419 DNA topoisomerases from NCLDVs⁵⁵. It will be interesting to test these enzymes as
420 alternative outgroups to root the eukaryotic tree. Our results indicate that further
421 digging into the diversity and molecular biology of NCLDV will probably have a major
422 impact on our understanding of the origin and early evolution of eukaryotes.



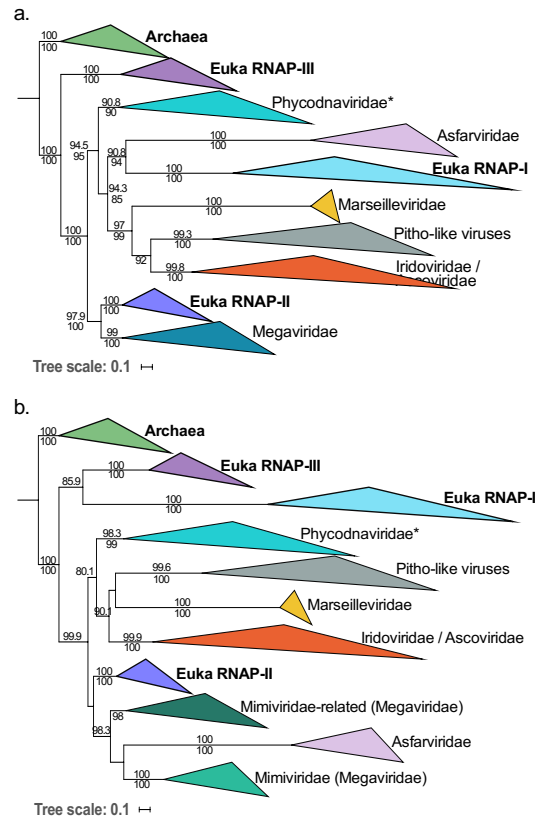
423
424 **Fig 1. Phylogenetic tree of the NCLDVs.** Bayesian inference (CAT-GTR model) of the
425 concatenated 8 core proteins from the NCLDVs after removal of *Poxviridae* and
426 *Aureococcus anophagefferens* virus. Genome sizes (in bp) are represented next to each
427 virus name. The scale-bar indicates the average number of substitutions per site. The
428 values at branches represent Bayesian posterior probabilities. Nodes without maximum
429 support are indicated in red.

430
431
432
433



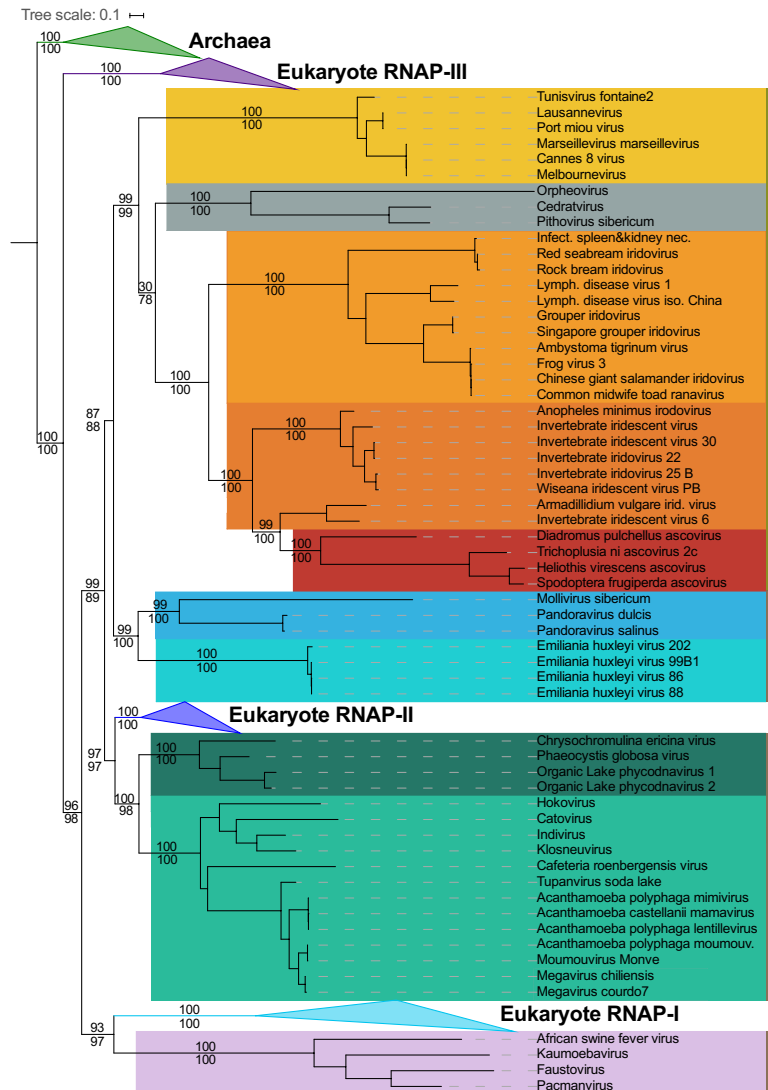
434
435 **Fig 2. Relationships between Polintoviruses and NCLDVs.** Maximum likelihood (ML)
436 phylogenetic tree of the concatenated structural proteins from Polintoviruses and
437 NCLDVs after removal of *Poxviridae* and *Aureococcus anophagefferens* virus. The scale-
438 bar indicates the average number of substitutions per site. The values at branches
439 represent support calculated by nonparametric bootstrap.

440
441
442

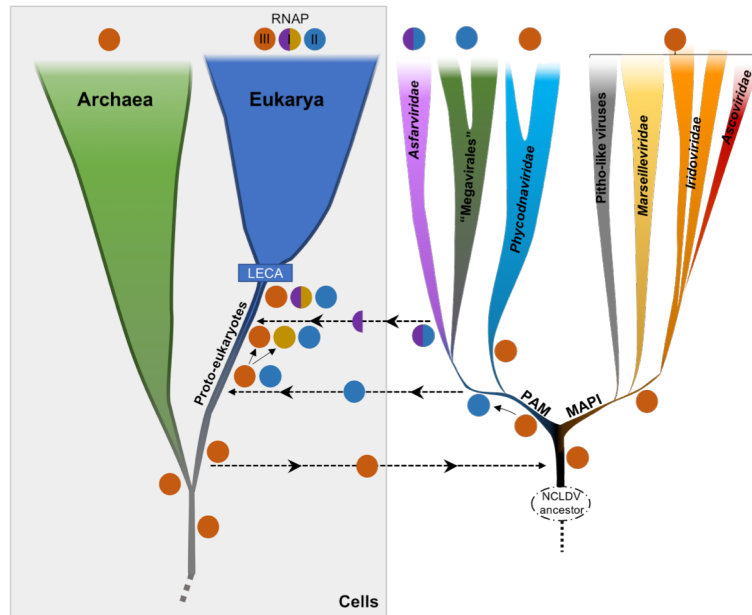


443
444
445
446
447
448
449
450
451
452

Fig 3. Maximum likelihood (ML) single-protein trees of the two largest RNA polymerase subunits from Archaea, Eukaryotes, and NCLDVs. ML phylogenetic trees of the RNAP-a (a) and RNAP-b (b) subunits, with Archaea used as the outgroup. The scale-bars indicate the average number of substitutions per site. Values on top and below branches represent support calculated by SH-like approximate likelihood ratio test (aLRT; 1,000 replicates) and ultrafast bootstrap approximation (UFBoot; 1,000 replicates), respectively. Only values superior to 80 are shown.



453
 454 **Fig 4. Maximum likelihood (ML) phylogenetic tree of the concatenated two largest**
 455 **RNAP subunits from Archaea, Eukaryotes, and NCLDVs.** ML phylogenetic tree of the
 456 concatenated of the two largest RNAP subunits, with Archaea used as the outgroup.
 457 Among the PAM superclade (light brown), “Megavirales”, *Asfarviridae*, and
 458 *Phycodnaviridae* are indicated in light/dark green, pink, and light/dark blue,
 459 respectively. Among the MAPI superclade (olive green), the *Marseilleviridae*, Pitho-like
 460 viruses, *Iridoviridae*, and *Ascoviridae* are indicated in dark yellow, grey, light/dark
 461 orange, and red, respectively. The scale-bar indicates the average number of
 462 substitutions per site. Values on top and below branches represent support calculated
 463 by SH-like approximate likelihood ratio test (aLRT; 1,000 replicates) and ultrafast
 464 bootstrap approximation (UFBoot; 1,000 replicates), respectively.
 465



466

467

468

469

470

471

472

473

474

475

Fig 5. Schematic representation of a putative scenario for the transfers of RNAP between cells and NCLDVs. An ancestral RNAP that later gave rise to the eukaryotic RNAP-III, actual ortholog of the archaeal RNAP, was transferred (at least the two largest subunits) from proto-eukaryotes to the ancestor of modern NCLDVs. A significantly divergent RNAP was later on transferred from the common ancestor of *Asfarviridae* and "Megavirales" to proto-eukaryotes. A new eukaryotic RNAP also emerged from a duplication event from the RNAP-III, before its largest subunit was replaced by that of *Asfarviridae*. These events occurred before LECA, the Last Eukaryotic Common Ancestor, that marked the emergence of modern eukaryotes.

476 **Methods**

477 **Datasets**

478 We initially collected a total of 96 NCLDV genomes from public databases
479 (Supplementary Table 2) that we used to build their core genome (see below). This
480 dataset comprises 17 Mimiviridae, 6 Marseilleviruses, 30 Iridoviridae, 4 Ascoviridae, 14
481 Poxviridae, 4 Asfarviridae, 15 Phycodnaviridae, 3 unclassified viruses (referred to as
482 Pitho-like viruses), 2 Pandoraviruses, 1 Mollivirus.

483 Preliminary phylogenetic analyses showed high redundancy within some groups
484 already comprising many members compared to others. We thus decided to remove
485 some genomes in order to obtain a more balanced sampling (Supplementary Table 2):
486 14 *Iridoviridae*, 2 *Phycodnaviridae* and 4 *Mimiviridae*. These analyses also revealed that
487 the *Poxviridae* on the one hand, and a single virus (*Aureococcus anophagefferens virus*)
488 on the other hand, always produce long branches and tend to change position in the tree
489 depending on the considered proteins or concatenation of proteins. We thus decided to
490 remove these viruses (14 *Poxviridae* and *Aureococcus anophagefferens virus*) from
491 subsequent analyses, leading to the dataset of 61 genomes used in the phylogenetic
492 analyses.

493 Ten polintoviruses sequences were collected from the Rebase collection⁵⁶
494 (http://www.girinst.org/Rebase_Update.html): Polinton-1_HM, Polinton-3_TC,
495 Polinton-5_NV, Polinton-2_NV, Polinton-1_DY, Polinton-1_TC, Polinton-1_SP, Polinton-
496 2_SP, Polinton-2_DR, Polinton-1_DR.

497 The cellular taxa included in some analyses were selected based on previous works
498 performed by some of us⁴⁴. The list of selected taxa is presented as Supplementary Table
499 4.

500

501 **Core genome building**

502 Because of the high divergence level of NCLDV genomes, we were not able to directly
503 identify genes shared among all of them. This is why we first started from two subsets of
504 NCLDVs, both being coherent enough and comprising enough members. Those two
505 subsets were the viruses annotated as *Mimiviridae* on the one hand and *Marseilleviridae*
506 on the other hand.

507 For each subset of genomes, we proceeded as follow. We defined groups of orthologous
508 genes by blasting one proteome against all the others. We only considered hits that had
509 an E-value less than $1e^{-10}$. We then identified pairwise reciprocal best hits with at least
510 20% similarity, and at least 40% of alignment coverage. We finally identified the union
511 of all the sets of orthologs and retained those present in more than half of the members
512 of the subset.

513 The result was two sets of orthologs, one for each subset of NCLDVs genomes. We
514 compared these two sets by identifying the matching proteins using BLAST and HMM
515 profiles and obtained orthologs found in both *Mimiviridae* and *Marseilleviridae*. Using
516 the aforementioned BLAST criteria, we checked for the presence of these orthologs in
517 other NCLDVs proteomes. When a protein was missing, we checked the presence of a
518 corresponding gene using TBLASTN to account for incomplete annotations of the
519 genomes, and also used HMM profiles to account for high sequence divergence. This
520 whole process resulted in a set of putative orthologous proteins found in all NCLDV
521 families.

522 In order to detect errors, typically different proteins assigned to the same group, we
523 used HMMer⁵⁷ to find a matching HMM profile in the PFAM database
524 (<http://pfam.xfam.org/>) for each group and discarded those significantly matching
525 more than one PFAM profile (after checking that these profiles were not from the same

526 protein family). We finally aligned the remaining orthologs and visually inspected the
527 alignments as a last control.

528 We obtained a list of orthologs that we ordered according to their presence in NCLDV
529 genomes to define different categories of core proteins.

530

531 **Phylogenetic analyses**

532 **Alignments**

533 All alignments were performed using MAFFT v7.397 and the E-INS-i algorithm⁵⁸, which
534 is designed to align sequences that are susceptible to contain large insertions. For one
535 RNA polymerase analysis (see manuscript), constraints in the alignments were used
536 with the seed option: independent alignments of each cellular clade (Archaea and the
537 three eukaryotic RNA polymerases) performed separately were used as constraints for
538 the global alignment. For the viral phylogenies, we trimmed each alignment of the
539 positions containing more than 20% of gaps using our own scripts. For the RNA
540 polymerase phylogenies with cellular sequences, the alignments were trimmed with
541 BMGE (with the -m BLOSUM30 and -b 1 options)⁵⁹.

542

543 **Maximum likelihood phylogenies**

544 Single-protein and concatenated protein phylogenies were conducted within the
545 Maximum Likelihood (ML) framework using IQ-TREE v1.6.3⁶⁰. We first performed a
546 model test with the Bayesian Information Criterion (BIC) by including protein mixture
547 models⁶¹. For mixture model analyses, we used the PMSF models⁶². The support values
548 were either computed from 100 bootstrap replicates in the case of nonparametric
549 bootstrap, or from 1,000 replicates for SH-like approximation likelihood ratio test
550 (aLRT)⁶³ and ultrafast bootstrap approximation (UFBoot)⁶⁴.

551

552 **Congruence analysis**

553 To detect potential incongruences within the signal carried by core proteins (after
554 removal of Poxviridae and Aureococcus anophagefferens virus) that could prevent their
555 global concatenation, we performed comparative phylogenetic analyses of every
556 possible combinations of 6 out of 8 core proteins through ML framework (see ML
557 method aforementioned). The 36 ML trees generated were carefully analyzed for
558 reference features estimated from the Bayesian phylogenetic tree (Fig 1), as well as from
559 most phylogenetic trees obtained throughout this study. The presence or absence of
560 these features were counted, and accordingly each feature was scored for its observed
561 frequency among the trees, as well as each tree was scored according to the number of
562 observed reference features (Supplementary Table 3).

563

564 **Supermatrix analysis**

565 We obtained a supermatrix by concatenating the 8 amino acid alignments of the core
566 genes. Supermatrices containing more characters, we computed ML trees with the
567 aforementioned method and performed Bayesian analyses using phyloBayes MPI
568 v1.5a⁶⁵ and the CAT-GTR model⁶⁶. Four independent chains were run until at least two
569 reached convergence with a maximum difference value <0.1 . The tree presented in Fig 1
570 was obtained from the convergence (maxdiff value: 0.097) of two chains of 3,426 and
571 3,276 generations. The first 25% of trees were removed as burn-in. The consensus tree
572 was obtained by selecting one out of every two trees. In order to account for
573 composition bias, we also applied two different character recodings, using 4 bins
574 according to two different binnings: the adaptation of the 6 Dayhoff groups⁶⁷ to 4 bins

575 proposed by Lartillot in phyloBayes manual, and the one proposed by Susko and
576 Rogers⁶⁸. For these analyses, a GTR+ Γ_4 +I model was used.

577

578 **Supertree analysis**

579 Horizontal gene transfers can deeply impact tree reconstruction when using alignment-
580 based methods. Supertree methods aim at reconciling sets of phylogenetic trees,
581 typically gene/protein trees, into an organismal tree even when such evolutionary
582 phenomena occur. Among the different proposed criteria for supertree methods, the
583 subtree prune-and-regraft (SPR) distance has proven to lead to more accurate tree
584 reconstructions⁶⁹. We used the software SPR Supertree v1.2.1⁶⁹ from the 8 single
585 protein phylogenies we previously inferred, after collapsing the clades for which the
586 support was less than 95%.

587

588 **Ancestral sequence reconstruction**

589 In order to try to reduce the risk of long branch attraction, we replaced, in the RNAP
590 tree, the eukaryotic clades by their ancestral sequences. These sequences were inferred
591 using IQ-TREE. We selected sites with a posterior probability greater than 0.7 and
592 replace the other sites by gaps.

593

594 **Topology test**

595 IQ-TREE v1.6.3 was used to perform Approximately Unbiased (AU) tree topology tests⁷⁰
596 for comparing the tree obtained with the concatenated RNAP genes (Fig 4) with two
597 other ones we built using the same methodology but constraining i) the monophyly of
598 the NCLDVs and ii) the monophyly of the cellular organisms. The AU tests rejected these
599 two new trees with p-values <1e-3.

600

601 Visualization

602 The phylogenetic trees were visualized with FigTree v1.4.3

603 (<http://tree.bio.ed.ac.uk/software/figtree/>) and iTOL⁷¹.

604

605

606 References

- 607 1. La Scola, B. *et al.* A Giant Virus in Amoebae. *Science* **299**, 2033–2033 (2003).
- 608 2. Claverie, J.-M. Viruses take center stage in cellular evolution. *Genome Biol.* **5** (2006).
- 609 3. Raoult, D. & Forterre, P. Redefining viruses: lessons from Mimivirus. *Nat. Rev.*
610 *Microbiol.* **6**, 315–319 (2008).
- 611 4. Moreira, D. & López-García, P. Ten reasons to exclude viruses from the tree of life.
612 *Nat. Rev. Microbiol.* **7**, 306–311 (2009).
- 613 5. Filée, J. & Chandler, M. Gene Exchange and the Origin of Giant Viruses. *Intervirology*
614 **53**, 354–361 (2010).
- 615 6. Forterre, P. Giant Viruses: Conflicts in Revisiting the Virus Concept. *Intervirology* **53**,
616 362–378 (2010).
- 617 7. Nasir, A., Forterre, P., Kim, K. M. & Caetano-Anollés, G. The distribution and impact of
618 viral lineages in domains of life. *Front. Microbiol.* **5**, 194 (2014).
- 619 8. Takemura, M., Yokobori, S. & Ogata, H. Evolution of Eukaryotic DNA Polymerases via
620 Interaction Between Cells and Large DNA Viruses. *J. Mol. Evol.* **81**, 24–33 (2015).
- 621 9. Forterre, P. & Gaïa, M. Giant viruses and the origin of modern eukaryotes. *Curr. Opin.*
622 *Microbiol.* **31**, 44–49 (2016).
- 623 10. Forterre, P. To be or not to be alive: How recent discoveries challenge the traditional
624 definitions of viruses and life. *Stud. Hist. Philos. Biol. Biomed. Sci.* **59**, 100–108 (2016).
- 625 11. Claverie, J.-M. & Abergel, C. Giant viruses: The difficult breaking of multiple
626 epistemological barriers. *Stud. Hist. Philos. Sci. Part C Stud. Hist. Philos. Biol. Biomed. Sci.* **59**,
627 89–99 (2016).
- 628 12. Koonin, E. V. & Krupovic, M. Polintons, virophages and transpovirons: a tangled web
629 linking viruses, transposons and immunity. *Curr. Opin. Virol.* **25**, 7–15 (2017).
- 630 13. Mihara, T. *et al.* Taxon Richness of ‘Megaviridae’ Exceeds those of Bacteria and
631 Archaea in the Ocean. *Microbes Environ.* **33**, 162–171 (2018).
- 632 14. Legendre, M. *et al.* Thirty-thousand-year-old distant relative of giant icosahedral DNA
633 viruses with a pandoravirus morphology. *Proc. Natl. Acad. Sci.* **111**, 4274–4279 (2014).
- 634 15. Philippe, N. *et al.* Pandoraviruses: Amoeba Viruses with Genomes Up to 2.5 Mb
635 Reaching That of Parasitic Eukaryotes. *Science* **341**, 281–286 (2013).
- 636 16. Iyer, L. M., Aravind, L. & Koonin, E. V. Common Origin of Four Diverse Families of
637 Large Eukaryotic DNA Viruses. *J. Virol.* **75**, 11720–11734 (2001).
- 638 17. Koonin, E. V. & Yutin, N. Nucleo-cytoplasmic Large DNA Viruses (NCLDV) of
639 Eukaryotes. in *eLS* (ed. John Wiley & Sons, Ltd) (John Wiley & Sons, Ltd, 2012).

- 640 18. Koonin, E. V., Krupovic, M. & Yutin, N. Evolution of double-stranded DNA viruses of
641 eukaryotes: from bacteriophages to transposons to giant viruses. *Ann. N. Y. Acad. Sci.* **1341**,
642 10–24 (2015).
- 643 19. Brussaard, C., Kempers, R., Kop, A., Riegman, R. & Heldal, M. Virus-like particles in a
644 summer bloom of *Emiliania huxleyi* in the North Sea. *Aquat. Microb. Ecol.* **10**, 105–113
645 (1996).
- 646 20. Boyer, M., Madoui, M.-A., Gimenez, G., La Scola, B. & Raoult, D. Phylogenetic and
647 phyletic studies of informational genes in genomes highlight existence of a 4 domain of life
648 including giant viruses. *PLoS One* **5**, e15530 (2010).
- 649 21. Yutin, N., Colson, P., Raoult, D. & Koonin, E. V. Mimiviridae: clusters of orthologous
650 genes, reconstruction of gene repertoire evolution and proposed expansion of the giant
651 virus family. *Viol. J.* **10**, 106 (2013).
- 652 22. Yutin, N. & Koonin, E. V. Pandoraviruses are highly derived phycodnaviruses. *Biol.*
653 *Direct* **8**, (2013).
- 654 23. Legendre, M. *et al.* Diversity and evolution of the emerging Pandoraviridae family.
655 *Nat. Commun.* **9**, (2018).
- 656 24. Moreira, D. & López-García, P. Evolution of viruses and cells: do we need a fourth
657 domain of life to explain the origin of eukaryotes? *Philos. Trans. R. Soc. B Biol. Sci.* **370**,
658 20140327 (2015).
- 659 25. Claverie, J.-M. & Abergel, C. Open Questions About Giant Viruses. in *Advances in*
660 *Virus Research* **85**, 25–56 (Elsevier, 2013).
- 661 26. Yutin, N. & Koonin, E. V. Hidden evolutionary complexity of Nucleo-Cytoplasmic Large
662 DNA viruses of eukaryotes. *Viol. J.* **9**, 161 (2012).
- 663 27. Andreani, J. *et al.* Cedratvirus, a Double-Cork Structured Giant Virus, is a Distant
664 Relative of Pithoviruses. *Viruses* **8**, 300 (2016).
- 665 28. Andreani, J. *et al.* Orpheovirus IHUMI-LCC2: A New Virus among the Giant Viruses.
666 *Front. Microbiol.* **8**, (2018).
- 667 29. Gallot-Lavallée, L., Blanc, G. & Claverie, J.-M. Comparative Genomics of
668 Chrysochromulina Ericina Virus and Other Microalga-Infecting Large DNA Viruses Highlights
669 Their Intricate Evolutionary Relationship with the Established Mimiviridae Family. *J. Virol.* **91**,
670 (2017).
- 671 30. Schulz, F. *et al.* Giant viruses with an expanded complement of translation system
672 components. *Science* **356**, 82–85 (2017).
- 673 31. Abrahão, J. *et al.* Tailed giant Tupanvirus possesses the most complete translational
674 apparatus of the known virosphere. *Nat. Commun.* **9**, (2018).
- 675 32. Reteno, D. G. *et al.* Faustovirus, an Asfarvirus-Related New Lineage of Giant Viruses
676 Infecting Amoebae. *J. Virol.* **89**, 6585–6594 (2015).
- 677 33. Klose, T. *et al.* Structure of faustovirus, a large dsDNA virus. *Proc. Natl. Acad. Sci.* **113**,
678 6206–6211 (2016).
- 679 34. Andreani, J. *et al.* Pacmanvirus, a New Giant Icosahedral Virus at the Crossroads
680 between Asfarviridae and Faustoviruses. *J. Virol.* **91**, (2017).
- 681 35. Bajrai, L. *et al.* Kaumobavirus, a New Virus That Clusters with Faustoviruses and
682 Asfarviridae. *Viruses* **8**, 278 (2016).
- 683 36. Oliveira, G. P., de Aquino, I. L. M., Luiz, A. P. M. F. & Abrahão, J. S. Putative Promoter
684 Motif Analyses Reinforce the Evolutionary Relationships Among Faustoviruses,
685 Kaumobavirus, and Asfarvirus. *Front. Microbiol.* **9**, (2018).

- 686 37. Bamford, D. H., Burnett, R. M. & Stuart, D. I. Evolution of Viral Structure. *Theor.*
687 *Popul. Biol.* **61**, 461–470 (2002).
- 688 38. Krupovic, M. & Bamford, D. H. Virus evolution: how far does the double beta-barrel
689 viral lineage extend? *Nat. Rev. Microbiol.* **6**, 941–948 (2008).
- 690 39. Abrescia, N. G. A., Bamford, D. H., Grimes, J. M. & Stuart, D. I. Structure Unifies the
691 Viral Universe. *Annu. Rev. Biochem.* **81**, 795–822 (2012).
- 692 40. Krupovic, M., Bamford, D. H. & Koonin, E. V. Conservation of major and minor jelly-
693 roll capsid proteins in Polinton (Maverick) transposons suggests that they are bona fide
694 viruses. *Biol. Direct* **9**, 6 (2014).
- 695 41. Krupovic, M. & Koonin, E. V. Polintons: a hotbed of eukaryotic virus, transposon and
696 plasmid evolution. *Nat. Rev. Microbiol.* **13**, 105–115 (2015).
- 697 42. Fischer, M. G. Giant viruses come of age. *Curr. Opin. Microbiol.* **31**, 50–57 (2016).
- 698 43. Filée, J., Forterre, P., Sen-Lin, T. & Laurent, J. Evolution of DNA Polymerase Families:
699 Evidences for Multiple Gene Exchange Between Cellular and Viral Proteins. *J. Mol. Evol.* **54**,
700 763–773 (2002).
- 701 44. Da Cunha, V., Gaia, M., Gadelle, D., Nasir, A. & Forterre, P. Lokiarchaea are close
702 relatives of Euryarchaeota, not bridging the gap between prokaryotes and eukaryotes. *PLoS*
703 *Genet.* **13**, e1006810 (2017).
- 704 45. Werner, F. & Grohmann, D. Evolution of multisubunit RNA polymerases in the three
705 domains of life. *Nat. Rev. Microbiol.* **9**, 85–98 (2011).
- 706 46. Da Cunha, V., Gaia, M., Nasir, A. & Forterre, P. Asgard archaea do not close the
707 debate about the universal tree of life topology. *PLOS Genet.* **14**, e1007215 (2018).
- 708 47. Yutin, N., Wolf, Y. I. & Koonin, E. V. Origin of giant viruses from smaller DNA viruses
709 not from a fourth domain of cellular life. *Virology* **466–467**, 38–52 (2014).
- 710 48. Filée, J. Route of NCLDV evolution: the genomic accordion. *Curr. Opin. Virol.* **3**, 595–
711 599 (2013).
- 712 49. Filée, J. Giant viruses and their mobile genetic elements: the molecular symbiosis
713 hypothesis. *Curr. Opin. Virol.* **33**, 81–88 (2018).
- 714 50. Eme, L., Spang, A., Lombard, J., Stairs, C. W. & Ettema, T. J. G. Archaea and the origin
715 of eukaryotes. *Nat. Rev. Microbiol.* **15**, 711–723 (2017).
- 716 51. Blombach, F. *et al.* Identification of an ortholog of the eukaryotic RNA polymerase III
717 subunit RPC34 in Crenarchaeota and Thaumarchaeota suggests specialization of RNA
718 polymerases for coding and non-coding RNAs in Archaea. *Biol. Direct* **4**, 39 (2009).
- 719 52. Takemura, M. Poxviruses and the Origin of the Eukaryotic Nucleus. *J. Mol. Evol.* **52**,
720 419–425 (2001).
- 721 53. Bell, P. J. Viral Eukaryogenesis: Was the Ancestor of the Nucleus a Complex DNA
722 Virus? *J. Mol. Evol.* **53**, 251–256 (2001).
- 723 54. Forterre, P. & Prangishvili, D. The Great Billion-year War between Ribosome- and
724 Capsid-encoding Organisms (Cells and Viruses) as the Major Source of Evolutionary
725 Novelties. *Ann. N. Y. Acad. Sci.* **1178**, 65–77 (2009).
- 726 55. Forterre, P., Gribaldo, S., Gadelle, D. & Serre, M.-C. Origin and evolution of DNA
727 topoisomerases. *Biochimie* **89**, 427–446 (2007).
- 728 56. Jurka, J. *et al.* Repbase Update, a database of eukaryotic repetitive elements.
729 *Cytogenet. Genome Res.* **110**, 462–467 (2005).
- 730 57. Eddy, S. R. Accelerated Profile HMM Searches. *PLoS Comput. Biol.* **7**, e1002195
731 (2011).

- 732 58. Katoh, K. & Standley, D. M. MAFFT multiple sequence alignment software version 7:
733 improvements in performance and usability. *Mol. Biol. Evol.* **30**, 772–780 (2013).
- 734 59. Criscuolo, A. & Gribaldo, S. BMGE (Block Mapping and Gathering with Entropy): a
735 new software for selection of phylogenetic informative regions from multiple sequence
736 alignments. *BMC Evol. Biol.* **10**, 210 (2010).
- 737 60. Nguyen, L.-T., Schmidt, H. A., von Haeseler, A. & Minh, B. Q. IQ-TREE: a fast and
738 effective stochastic algorithm for estimating maximum-likelihood phylogenies. *Mol. Biol.*
739 *Evol.* **32**, 268–274 (2015).
- 740 61. Kalyaanamoorthy, S., Minh, B. Q., Wong, T. K. F., von Haeseler, A. & Jermiin, L. S.
741 ModelFinder: fast model selection for accurate phylogenetic estimates. *Nat. Methods* **14**,
742 587–589 (2017).
- 743 62. Wang, H.-C., Minh, B. Q., Susko, E. & Roger, A. J. Modeling Site Heterogeneity with
744 Posterior Mean Site Frequency Profiles Accelerates Accurate Phylogenomic Estimation. *Syst.*
745 *Biol.* **67**, 216–235 (2018).
- 746 63. Guindon, S. *et al.* New Algorithms and Methods to Estimate Maximum-Likelihood
747 Phylogenies: Assessing the Performance of PhyML 3.0. *Syst. Biol.* **59**, 307–321 (2010).
- 748 64. Minh, B. Q., Nguyen, M. A. T. & von Haeseler, A. Ultrafast Approximation for
749 Phylogenetic Bootstrap. *Mol. Biol. Evol.* **30**, 1188–1195 (2013).
- 750 65. Lartillot, N., Lepage, T. & Blanquart, S. PhyloBayes 3: a Bayesian software package for
751 phylogenetic reconstruction and molecular dating. *Bioinforma. Oxf. Engl.* **25**, 2286–2288
752 (2009).
- 753 66. Lartillot, N. & Philippe, H. A Bayesian mixture model for across-site heterogeneities in
754 the amino-acid replacement process. *Mol. Biol. Evol.* **21**, 1095–1109 (2004).
- 755 67. Embley, T. M., van der Giezen, M., Horner, D. S., Dyal, P. L. & Foster, P. Mitochondria
756 and hydrogenosomes are two forms of the same fundamental organelle. *Philos. Trans. R.*
757 *Soc. Lond. B. Biol. Sci.* **358**, 191–201–202 (2003).
- 758 68. Susko, E. & Roger, A. J. On reduced amino acid alphabets for phylogenetic inference.
759 *Mol. Biol. Evol.* **24**, 2139–2150 (2007).
- 760 69. Whidden, C., Zeh, N. & Beiko, R. G. Supertrees Based on the Subtree Prune-and-
761 Regraft Distance. *Syst. Biol.* **63**, 566–581 (2014).
- 762 70. Shimodaira, H. An Approximately Unbiased Test of Phylogenetic Tree Selection. *Syst.*
763 *Biol.* **51**, 492–508 (2002).
- 764 71. Letunic, I. & Bork, P. Interactive tree of life (iTOL) v3: an online tool for the display
765 and annotation of phylogenetic and other trees. *Nucleic Acids Res.* **44**, W242–245 (2016).
- 766